SILVER NANOPARTICLES INDUCE APOPTOSIS IN L5178Y LYMPHOMA BY LIPOPEROXIDE ACTIVITY

I. YAÑEZ-SÁNCHEZ[a], C. DE LA LUZ CARREÓN-ÁLVAREZ[b],
C. VELÁSQUEZ-ORDÓÑEZ[a], M. L. OJEDA-MARTÍNEZ[a],
F. JAVIER GÁLVEZ-GASTÉLUM[c], A. ZAMUDIO-OJEDA[d],
E. GERMÁN CARDONA-MUÑOZ[c], T. GARCÍA-IGLESIAS[e]*
aCentro de Investigación en Nanociencias y Nanotecnología, Depto. Ciencias Naturales y Exactas, Centro Universitario de los Valles, Universidad de Guadalajara, Carr. Guadalajara-Ameca Km. 45.5, C.P. 46600, Ameca, Jalisco, México
bDepto. Electrónica y computación, Centro Universitario Ciencias Exactas e Ingenierías, Universidad de Guadalajara, Blvd Gral. Marcelino García Barragán 1421, Olímpica, 44430 Guadalajara, Jalisco, México
cInstituto de Investigación Terapeutica Experimental y Clínica, Depto. Fisiología, Centro Universitario de Ciencias de la Salud, Universidad de Guadalajara, Sierra Mojada 950, Col. Independencia, C.P. 44340, Guadalajara, Jalisco, México
d.Depto. Física, Centro Universitario Ciencias Exactas e Ingenierías, Universidad de Guadalajara, Blvd Gral. Marcelino García Barragán 1421, Olímpica, 44430, Jalisco, México
eLaboratorio de Inmunología, Depto. Fisiología, Centro Universitario de Ciencias de la Salud, Universidad de Guadalajara, Sierra Mojada 950, Col. Independencia, C.P. 44340, Guadalajara, Jalisco, México

The use of nanomaterials for cancer treatment is not a new concept, but the ability to kill the cells without harming surrounding healthy cells has significant potential. The field of nanomedicine is concerned with technology based on the development of materials at the nanometric scale. In this paper, apoptosis/proliferation and lipid peroxide activity were evaluated in L5178Y lymphoma cells after exposure of Ag nanoparticles (NPs) to different concentrations of nanomaterials. Ag-NPs showed absorption at 412 nm, with a diameter of 2–9 nm. The treatment of L5178Y lymphoma cells with Ag-NPs demonstrated a significant decrement in the cellular proliferation index at 9 μg/mL; this result was supported with apoptosis determination, because at higher concentrations (>9 μg/mL) of Ag-NPs we observed the maximum peaks. With regard to the apoptotic mechanism of the effects of Ag-NPs on cell viability, we evaluated the lipoperoxide activity, which showed an important increment at the same concentration of Ag-NPs (9–18 μg/mL). We demonstrated that L5178Y lymphoma cells showed apoptosis induced by treatment with Ag-NPs; the possible mechanism of this effect could be the generation of lipoperoxides. Our study provides evidence for a molecular mechanism of Ag-NP-induced generation of reactive oxygen species (ROS).

*Corresponding author: trini.iglesias@gmail.com

1. Introduction

The convergence of nanotechnology with medicine (nanomedicine) has added new hope in the therapeutic and pharmaceutical field [1]. This new field of nanoscience has raised the possibility of using therapeutic nanoparticles in the diagnosis and treatment of cancer. In particular, silver nanoparticles (Ag-NPs) have proven to be good candidates for the treatment of this disease [2] because of their unique biologic effects that are based on their structure and size, allowing the creation of new mechanisms for treatment that differ from those of traditional drugs. Ag-NPs and ions have been shown to possess intrinsic cytotoxic activity [3].

Several studies have demonstrated that uptake of Ag-NPs by cells occurs via endocytosis and clathrin-mediated macropinocytosis, suggesting that cancer cells are susceptible to these Ag-NPs, as it has been reported that Ag-NPs act via ROS production and glutathione depletion in rat liver cells [1,4]. Similarly, Rahman *et al*. observed an upregulation of oxidative stress response genes (superoxide dismutase 2, glutathione reductase-1, etc.) in mouse brain following exposure to Ag-NPs [5].

Lymphoma is the term used to describe a group of blood cancers that develop in the lymphatic system. Hodgkin and non-Hodgkin are the two main types of lymphoma. Experimental models for the study of this type of cancer have been developed, for example L5178Y mouse lymphoma cells, which are used as a cellular system suitable for assessing the mutagenic, clastogenic, aneugenic, and genotoxic (DNA-damaging activity) properties of various agents [6,7].

The occupational hazard associated with nanoparticle (NP) exposure and the molecular mechanisms underlying Ag-NP toxicity are still unknown; however, our aim was to determine the cytotoxic effects (in proliferation/apoptosis) of Ag-NPs on L5178Y lymphoma under *in vitro* conditions.

2. Experimental procedures

Synthesis of colloidal silver nanoparticles

Ag-NP solutions were prepared using 0.1 g of silver nitrate ($AgNO_3$) in 100 ml of ethanol and 1 g polyvinyl-pyrrolidone (PVP) as a stabilizing agent, with a weight ratio of 1:10 silver nitrate:PVP. The ethanolic solution containing the metallic salt and PVP was refluxed to 363 K and stirred for a period of 12 h [8]. The formation of Ag-NPs could be observed at a glance by a change in colour in the solution, since small Ag-NPs are amber. The addition of a small amount of PVP prevented aggregation of Ag particles.

Characterization techniques

After the Ag-Np synthesis and various days afterwards, small sample aliquot diluting into ethanol was analysed by Ultraviolet-Visible (UV-Vis) spectrophotometry (UV-Vis spectrophotometer UV-Vis cary 300).

Transmission Electron Microscope (TEM): Samples for TEM analysis were analysed with a JEM-2010F FASTEM electron microscope operating at 300 kV. The samples were prepared by dissolving in ethanol, and were next deposited on 300 mesh Cu grids and subsequently dried in air before being analysed by TEM.

Exposure to Ag-NPs

To experimentally study the effect, we obtained L5178Y murine lymphoma cells from an *in vivo* culture of DBA2 mouse. These were washed twice with phosphate-buffered saline (PBS) (SIGMA^{TM}) and the supernatant was decanted. Cellular viability was determined by trypan blue exclusion and quantified in a Neubauer camera. Cells were adjusted to 1×10^5/mL in RPMI-1640 medium (GIBCO^{TM}) and were collocated in each well on the plate in the absence/presence of Ag-

NPs 1.74×10^{-3} at different concentrations (4.5 to 72 µg/mL). Then, the plate was incubated at 37 °C with 95% relative humidity and 5% CO_2 atmosphere for 24 h.

Proliferation assay

The CPI was obtained by a modification of the original Mossman technique involving metabolic reduction of MTT (3-(4, 5-dimethylthiazol-2-ilo)-2,5-difeniltetrazol bromide) [9,10]. After Ag NP stimulation, MTT (SIGMA™) and extraction buffer (20% sodium dodecyl sulfate (SIGMA™) and 50% dimethyl formamide (SIGMA™)) were added. The plate was incubated for 24 h and read at 570/630 nm in an ELISA reader (Synergy HT Multi-Mode Microplate Reader, with software Gen5 v2.0, Biotek), and the CPI was calculated as the ratio of the optical density of wells with mitogen to that of wells without mitogen.

Apoptosis determination

After Ag-NP stimulation, the cells were washed twice with PBS and 5 µL of FITC-Anexin V was added, after which the cells were incubated for 15 min. Then, 5µL of propidium iodide was added to enable the evaluation of apoptosis by a detection kit (BD Pharmigen™). Finally, apoptotic cells were measured on an EPICS XL-MCL Flow Cytometer (Beckman Coulter, Krefeld, Germany). The results were expressed in percentages.

Lipoeroxide activity

To evaluate the lipoperoxide activity, the cell culture supernates of cells stimulated with or without Ag NPs for 24 h were collected. We performed a colorimetric high-sensitivity assay using a commercial kit (Kamiya Biomedical Company) in accordance with the manufacturer's instructions. Finally, the plate was read at 675 nm in the ELISA reader. Lipoperoxide (LPO) activity was calculated by the formula LPO = ((ODs – ODb) x 50) / (ODcal – ODb), where ODs is sample optical density, ODb is blank optical density, and ODcal is a calibrator of 50nmol/mL optical density.

Statistical analysis

The nonparametric Mann–Whitney U test was used to compare differences of medians in the CPI between the experimental and control groups. The other variables were evaluated by ANOVA. Statistical significance was set at $p<0.05$. All analyses were performed using IBM® SPSS® statistics version 20.

3. Results and discussion

The biological risk of using Ag-NPs in humans has not been clearly established. Because of their small size, it is difficult for NPs to find a biological barrier that might obstruct their passage and deposition onto various tissues. Also, their interaction with different biomolecules has not been fully established [11].

Ag-NP characterization

The ultraviolet visible (UV-Vis) spectra of Ag-NPs synthetized and used in *in vitro* experiments show an absorption peak at 412 nm, which indicates the presence of typical Ag in the sample (Fig. 1A). TEM images clearly indicated the presence and size of particles, which consist of small NPs with sizes between 2–9 nm (Fig. 1B). The composition of the synthetized samples was determined using energy dispersive X-ray spectroscopy (EDX). In the spectrum showing the

signals of Cu and Ag (Fig. 1C), the Cu signal originates from the grid used for microscopy and the Ag signal originates from the NPs.
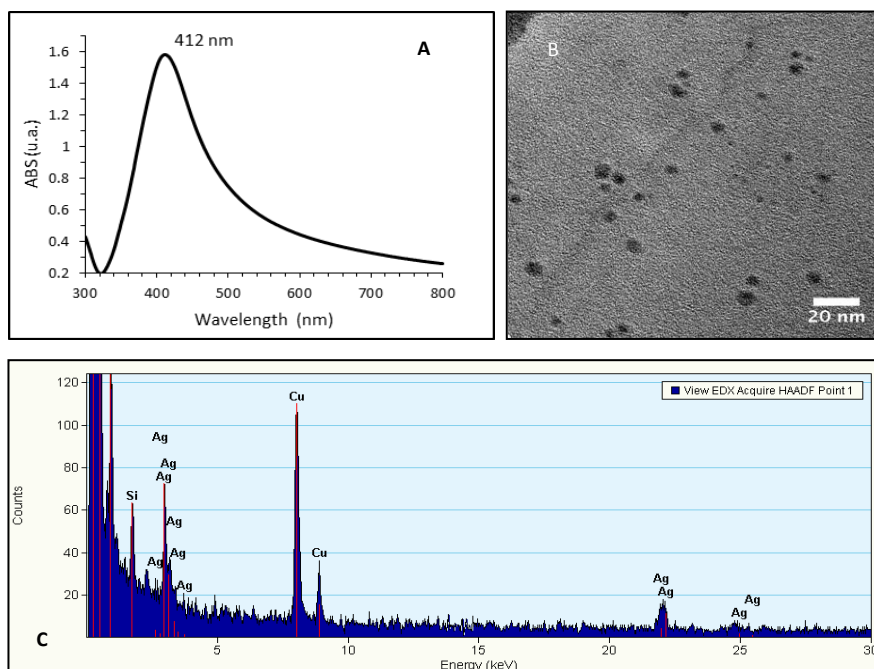
Fig. 1. Ag NP characterization. A) UV-Vis spectra. B) High-resolution TEM (HRTEM) image showing the size and morphology of the Ag NPs. C) Chemical analysis of Ag NP synthesis by Energy Dispersive X-ray (EDX).

In the visible range, Ag-NPs exhibit optical properties different from those of the bulk material. This is because of their size and shape, and the control of particle size and morphology enables certain flexibility in creating new types of nanostructures [12] with a degree of control over their physical and chemical properties. The Ag colloids are very small, resulting in a large available surface area and possible penetration to the cell cytoplasm and nucleus, it like as carrier for gene delivery. Nanometer-size Ag colloids have a large available surface area and a very small size, which allows the penetration of such materials to the cell cytoplasm and nucleus [13].

Cellular proliferation index

The cell viability assay is one of the most important methods for toxicology analysis. It explains the cellular response to toxic materials and can provide information on cell death, survival, and metabolic activities. In our experiment, the cells were treated with various concentrations of Ag-NPs for 24 h. The results suggest that these NPs could reduce the cellular proliferation index (CPI) of L5178Y lymphoma cells in a dose-dependent manner. After 24 h of treatment, it was found that the Ag-NPs were cytotoxic to the cells at concentrations of 9 μg/mL and higher (Fig. 2).

The CPI shows a dual profile effect at different concentrations (Fig. 2). Despite than with vehicle was observed the maximum peak; it should be a proliferative effect on the cells by Ag-NP agglomerates [14].
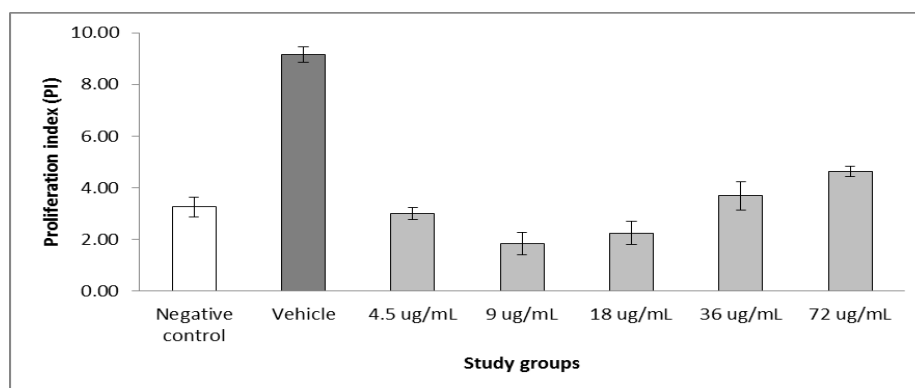
*Fig. 2. The cellular proliferation index, showing a dual dose-dependent effect of Ag NPs,
with statistical significance at 0.03, 0.25 mg concentrations*

The results of the proliferation test show an important increase in proliferation in our vehicle test group. However, in the sets of cells stimulated with Ag-NPs, a low proliferation was observed, which leads us to consider that the vehicle may have a proliferative effect on the cells or that Ag-NPs may be agglomerating and, somehow, creating an antiproliferative effect. With that in mind, J. Jiménez (2007) assessed the *in vitro* compatibility of polymers such as polyvinylpyrrolidone (PVP), which in proliferation tests shows cell growth levels exceeding 90%, quite similar to those in the control, and an absence of PVP cytotoxicity in the cells [14].

In previous studies, Ag NPs have been proven to avoid proliferation through the induction of apoptosis by liberating free radicals [1,15]. Several methodologies, such as MTS, MTT and BrUd, are used to measure the CPI, all with a similar biochemical base. We decided to use the MTT procedure because this technique permits evaluation of the mitochondrial oxidative-reduction process by Cyt p450 oxidation and succinate dehydrogenase (NADPH), with the conversion producing formasan crystals. This reaction could generate fat acid lipids and activate lipoperoxide activity [16].

A new cytological characteristic was observed in NP-treated cells, namely the radial organization of the culture following the formation of grooves (data not shown). This could be caused by disturbances in cytoskeletal functions as a consequence of NP treatment [17]. Similar observations have been reported by other groups, including the assembly of endothelial cells into linear arrangements using magnetic NPs [18]. Our research group is working to elucidate the molecular mechanism of these results.

Apoptosis

The results of the annexin V/PI assay showed a significant reduction in the percentage of viable cells after 24 h of exposure to Ag-NPs. Compared with the negative control, a significant increase in apoptosis, measured as annexin V-positive cells, was seen at doses of Ag-NPs ≥18 μg/mL, and, similar to the positive control, we did not find changes at higher concentrations (18, 36 and 72 μg/mL) of Ag NPs (Fig. 3).
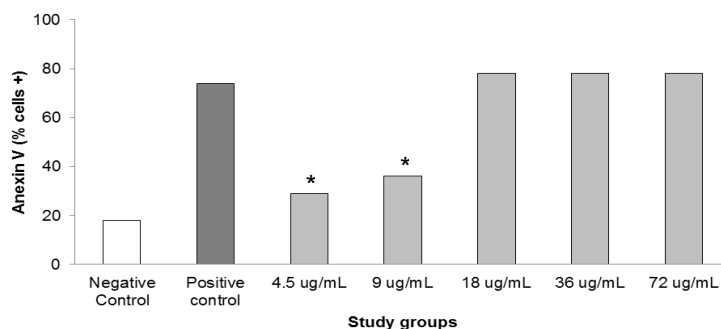
1686

*Fig. 3. Percentage of apoptotic cells. The apoptosis was maintained at 18 μg/mL of Ag NPs above the positive control * p <0.05.*

In our study, we observed that apoptosis was present at >9 μg/mL of Ag-NPs in L5178Y Lymphoid, and these results support the hypothesis that Ag-NPs may be used as an apoptotic agent [19].

Apoptosis has been described as "programmed cell death," and can be induced by elevated concentrations of ROS. ROS production triggers caspase activity in cytoplasmic cells, a process in which mitochondria play an important role, because they are the major sites of ROS production. AshaRani has reported that fibroblast exposed to Ag-NPs had toxicity through intracellular calcium (Ca^+) to activate oxidative-reduction reactions to produce Ag^+ ions (oxidative stress); it has been proposed that these ions may cause DNA damage [1].

Lipoperoxide quantification

To further investigate the induction of oxidative stress, we performed a colorimetric high-sensitivity assay using a commercial kit as a surrogate marker of lipid peroxidation and observed an important effect of Ag-NPs (9–18 μg/mL) on the generation of lipid peroxides (Fig. 4). Nevertheless, at higher concentrations, the activity of these lipoperoxides decreased.
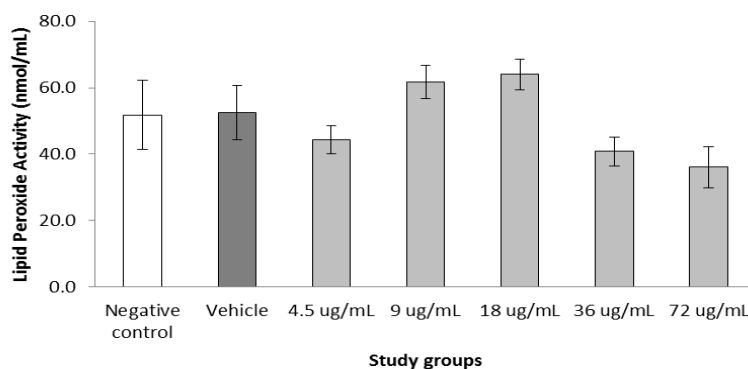

Fig. 4. Lipoperoxide activity in supernates of test groups. A dual Ag-NP dose-dependent profile concentration was observed.

To highlight ROS production, we performed lipid peroxidation experiments. The oxidation of fatty acids leads to the generation of lipid peroxides, thereby initiating a chain reaction that results in the disruption of the plasma and organelle membranes and subsequent cell death [20], in particular in the mitochondrion-mediated apoptosis pathway [21].

Lipoperoxide activity was increased in the lymphoma cells stimulated with Ag-NPs, and these results could be associated with ROS production and disruption of membranes in apoptotic cells [1].

4. Conclusion

In conclusion, the Ag-NPs that were synthetized by chemical reduction, controlling their size and morphology, presented proapoptotic effects at low concentrations in L5178Y lymphoma cells with incremental lipoperoxide activity. The findings of this study suggest the potential of Ag-NPs in the development of drugs to combat cancer. Nonetheless, further studies related to the cytotoxicity of Ag-NPs are needed in order to understand their secondary effects on healthy systems.

References

[1] P. V AshaRani, M. H. Prakash, S. Valiyaveettil. BMC Cell Biology **10**, 65 (2009).
[2] M. I.Sriram, S. B. Mani-Kanth, K. Kalishwaralal, S. Gurunathan, Int J Nanomedicine **5**, 753 (2010).
[3] J. S. Kim, E. Kuk, K.N. Yu, J.H. Kim, S.J. Park, H.J. Lee, S.H. Kim, Y.K. Park, Y.H. Park, C.Y. Hwang, Y.K. Kim, Y.S. Lee, D.H. Jeong, D.H. Cho Nanomedicine **3**, 95 (2007).
[4] S.M. Hussain, K.L. Hess, J.M. Gearhart, K.T. Geiss and J.J. Schlager. Toxicol in Vitro **19,** 975 (2005).
[5] M.F. Rahman, J. Wang, T.A. Patterson, U.T. Saini, B.L. Robinson, G.D. Newport, R.C. Murdock, J.J. Schlager, S.M. Hussain and S.F. Ali. Toxicol Lett **187,** 15 (2009).
[6] H. Stopper, S.O. Muller. Toxicol In Vitro. **11,** 661 (1997).
[7] S.O. Muller, I. Eckert, W.K. Lutz and H. Stopper. Mutat Res **371,** 165 (1996).
[8] J.S. Kim, J Ind Eng Chem. **13,** 566 (2007).
[9] T. Mosmann. J Immunol Methods **65**, 55 (1983).
[10] F. Denizot and R. Lang. J Immunol Method **89,** 271 (1986).
[11] A. Villegas Ph. D Thesis. Escuela Nacional de Medicina y Homeopatía, Instituto Politécnico Nacional, 2009.
[12] K. Jong-Seok. J. Ind. Eng. Chem **13,** 566 (2007).
[13] M.J. Clift, B. Rothen-Rutishauser, D.M. Brown, R. Duffin, K. Donaldson, L. Proudfoot, K. Guy and V. Stone, Toxicol Appl Pharmacol **232,** 418 (2008).
[14] J. Jiménez, N. Gonzalez, M. Fernandez, C. Elvira, A. López and J. San Roman. Biomecánica. **15,** 63 (2007).
[15] P.V. AshaRani, S. Sethu, H.K. Lim, G. Balaji, S. Valiyaveettil, M.P. Hande. Genome Integr **3,** 2 (2012).
[16] P.V. AshaRani, G.L. Kah-Mun, M.P. Hande and S. Valiyaveettil. ACS Nano **3,** 279 (2009).
[17] N. Pernodet, X. Fang, Y. Sun, A. Bakhtina, A. Ramakrishnan, J. Sokolov, A. Ulman, M. Rafailovich. Small **2,** 766 (2006).
[18] M.D. Krebs, R.M. Erb, B.B. Yellen, S. Bappaditya, B. Avinash, V.M. Rotello and A. Eben. Nano Lett **9,** 1812 (2009).
[19] H.H. Lara, N.V. Ayala-Nuñez, L. Ixtepan-Turrent and C. Rodriguez-Padilla. J Nanobiotechnology **8,** 1 (2010).
[20] Y. Wang, X.Y. Zi, J. Su, H.X. Zhang, X.R. Zhang, H.Y. Zhu, J.X. Li, M. Yin, F. Yang Y.P. Hu. Int J Nanomedicine **7,** 2641 (2012).
[21] Y. Wang, F. Yang, H.X. Zhang, X.Y. Zi, X.H. Pan, F. Chen, W.D. Luo, J.X. Li, H.Y. Zhu Y.P. Hu. Cell Death and Disease **4,** e783 (2013).